# Optimization, characterization, and evaluation of carrageenan/alginate/poloxamer/curcumin hydrogel film as a functional wound dressing material

Katarina Postolović [a], Biljana Ljujić [b], Marina Miletić Kovačević [c], Slađana Đorđević [a], Sandra Nikolić [b], Suzana Živanović [d], Zorka Stanić [a],*

[a] University of Kragujevac, Faculty of Science, Department of Chemistry, Serbia
[b] University of Kragujevac, Faculty of Medical Sciences, Department of Genetics, Serbia
[c] University of Kragujevac, Faculty of Medical Sciences, Department of Histology and Embryology, Serbia
[d] University of Kragujevac, Faculty of Medical Sciences, Department of Dentistry, Serbia

ABSTRACT

Curcumin belongs to a group of multipurpose drugs that can enhance the wound healing process. In this paper, films based on natural polysaccharides - κ-carrageenan and alginate - were prepared with added synthetic polymer poloxamer 407 to use these carriers for curcumin encapsulation and further apply them in wound healing. The film preparation process (film composition, components ratio, and crosslinking time) has been optimized. Curcumin, as a drug model, has been incorporated into optimal films. Structure, morphology, thermal properties, and the crystallinity degree of optimal films were determined using infrared spectroscopy, scanning electron microscopy, thermogravimetric analysis, and X-ray diffraction method. The *in vitro* release of curcumin from films was monitored for 24 h, achieving its cumulative release with a maximum release rate of 87.64%. The formation of complexes based on carrageenan, alginate, and poloxamer and the interaction of these complexes with curcumin were studied using theoretical models, AIM and NBO analysis. The effect of prepared films on cell viability was also examined. Films with incorporated curcumin were found to accelerate wound healing, both in *in vitro* and *in vivo* conditions, indicating their potential as new transdermal wound healing systems.

## 1. Introduction

Skin changes (wound, defect, or injury) occur as a result of various mechanical tissue damages (sting, cut, blow) or burns caused by high temperatures or chemicals [1]. As a specific biological process, wound healing refers to tissue growth and regeneration. The wound healing process is usually divided into five phases (hemostasis, inflammation, migration, proliferation, and maturation), during which complex biochemical and cellular reactions take place [1–3]. After the end of the hemostatic phase, fluid called exudate is formed from the wound, and it is present in all further phases in the healing process [4]. The formed exudate is one of the key factors in the healing process. It creates an ideal environment for effective and efficient healing (exudate allows the transfer of nutrients to the wound and creates conditions that allow the migration of epithelial cells). However, if excess exudate is formed, complications can occur during the healing process. For this reason, one of the main characteristics wound healing carriers should have is the ability to remove excess exudate, but also to maintain wound moisture at the required level [5].

Numerous studies have developed different formulations incorporating various bioactive molecules that positively affect different wound healing phases [1,6,7]. Current studies focus on developing new solid formulations with the biological activity of the constituents or incorporated drugs that can cover the wound and remain unchanged for a long time [8–14]. Composite hydrogel films based on natural polysaccharides, as materials able to form hydrogel, are widely used in biomedicine [10,15–18]. Combining polysaccharides can enhance the film mechanical properties and swelling degree because of possible beneficial synergistic effects [8,15–18]. Elastic hydrogel films containing targeted drugs are widely used in the skin wound healing process [8–11,15–19]. Although carriers are dry and solid, when they come into contact with the moist wound surface environment, the wound exudate passes into the polymer matrix, causing carrier hydration (swelling) [20]. Swelling of the carrier increases the distance between the polymer chains and creates a system that can release bioactive components to the wound [20].

Carrageenan is an anionic sulfonated polysaccharide (consisting of glycoside-linked galactose and anhydrogalactose) obtained by extraction from specific types of red algae [21]. There are many formulations containing carrageenan that can be used for different drug administration: oral, through the buccal mucosa, nasal, ocular, transdermal [22]. Hydrogel-based formulations with carrageenan as a component can be used in wound healing thanks to excess fluid absorption and biocompatibility properties. Good wound healing results (not only *in vitro,* but also *in vivo*) are achieved by encapsulation of various bioactive components in κ or ι-carrageenan-based formulation [22]. Very high encapsulation percentages of low soluble and bioavailable drugs can be achieved by chemical modification of carrageenan or preparing formulations containing polymer blends [21].

Alginates are salts of alginic acid (composed of chains of D-mannuronic and L-guluronic acid) isolated from brown algae [23]. They are mainly found as soluble salts, of which sodium alginate is the most used. As a polysaccharide with a large number of hydroxyl and carboxyl groups, alginate is a hydrophilic biopolymer that is non-toxic, biocompatible, stable under physiological conditions, and biodegradable [24]. These characteristics make alginates suitable for use primarily in the pharmaceutical industry in preparing various biomedical formulations. Alginate-based hydrogel with the most favorable properties is formed in the presence of divalent and multivalent metal ions, especially calcium ions [25]. The crosslinking of alginates, which is formed by the interaction of guluronic acid chains and calcium ions, is best described through the "*egg-box*" model [26]. Alginates have also been widely applied in preparing formulations used for wound healing due to their compatibility with human tissue [26]. It was demonstrated that proper selection of the alginate concentrations can yield tissue adhesives with desired bonding strengths and physical properties which enable further use of prepared formulations for various medical applications [27–29]. Alginate-based dressings offer good balance between cytotoxicity and bonding strength due to their composition because they can mimic the same process that naturally occurs during the blood coagulation [27–29]. Chemical modifications of available alginate hydroxyl and carboxyl groups or copolymerization of alginate with other compounds can improve alginate formulation properties and achieve higher drug encapsulation rates and desired release kinetics [30]. It has been noticed that hydrogel film, based on κ-carrageenan, in the presence of Na-alginate could be a potential topical wound dressing material [18].

Poloxamers, commercially known as Pluronic®, are formed by polymerization of ethylene oxide (EO) with propylene oxide (PO) [31]. Depending on polymerization degree and the corresponding monomer units ratio (EO/PO), different types of poloxamers can be obtained - poloxamers 188, 407, 68, and many others [31,32]. Poloxamer 407, also commercially known as Pluronic F127, is a nonionic surfactant [32]. As a surfactant, poloxamer can build micelles at concentrations/temperatures above the critical micellar concentration/temperature [33,34]. Therefore, adding poloxamer 407 can increase hydrophobic drug solubility. Thanks to the poloxamer hydrogel-forming ability, this surfactant is also used in formulations for wound healing [35].

Curcumin belongs to a class of hydrophobic polyphenolic compounds known as curcuminoids [36,37]. Curcumin has antioxidant, anticancer, anti-inflammatory, and antimicrobial properties [36,37]. However, despite high efficacy and beneficial properties, the use of curcumin is limited due to its very low bioavailability caused by its hydrophobic nature [38]. Therefore, many studies have investigated the preparation of formulations that can increase curcumin bioavailability [38,39].

Curcumin and it's derivatives have good potential for use in wound healing due to its anti-inflammatory and antioxidant properties [40,41]. It is also known that curcumin can improve wound healing as it participates in the processes of granulation tissue formation, damaged tissue regeneration, and collagen deposition [40,42]. Research results [42] indicate that the use of curcumin in wound healing improves epithelial

cell regeneration and can increase the proliferation of fibroblasts.

Considering the properties of carrageenan and alginate (natural saccharides), poloxamer 407 (surfactant), and curcumin (drug), in this paper was optimized the composition of films with these components to increase the bioavailability of curcumin. Additionally, besides optimizing the composition of films and films characterization, this study also explored interactions between components using theoretical models. Finally, potential applications of prepared films were investigated during the wound healing process under *in vivo* conditions.

## 2. Materials and methods

### 2.1. Materials

Sodium alginate and κ-carrageenan were obtained from Roth. Curcumin, poloxamer 407, calcium chloride dihydrate, potassium chloride, sodium chloride, glutamine, fetal bovine serum, penicillin, streptomycin, MTT, trypan blue, ketamine, and xylazine were purchased from Sigma-Aldrich. Glycerol and ethanol were obtained from Honeywell. Sodium hydrogen phosphate dihydrate was purchased from Poch and potassium dihydrogen phosphate from Kemika. Non-essential amino acids were obtained from Capricorn Scientific GmbH.

### 2.2. Film preparation

Polymer-based films were prepared using the solvent-casting process in a two-stage crosslinking procedure by modification of procedures described in the literature [43,44]. In the first stage, adequate amounts of polysaccharides were added to distilled water that already contains glycerol as a plasticizer. The mixture of polysaccharides (1.5–3.0%, w/w) and glycerol was stirred (500 rpm) at room temperature. After 1 h, the mixture temperature was raised to 70 ºC, the stirring rate was increased to 1000 rpm (to avoid local gelation), and a calcium chloride solution (0.5% w/w) was added dropwise (1 mL/min) to the mixture. After adding the CaCl$_2$ solution, stirring was continued for 20 min under the same conditions. The following step was sonication to homogenize the mixture. Then, the mixture was poured into Petri dishes (d=9 cm) and dried for 20 h at a temperature of 40 ºC. The films obtained after the drying process were partially crosslinked films. In the second phase, to achieve full crosslinking, the dried partially crosslinked films were immersed in a 10% glycerol and 3% calcium chloride solution. After crosslinking, excess glycerol and calcium chloride was removed from the film surface by rinsing with distilled water. The edges of the rinsed films were tightened with Teflon rings to prevent film deformations. Finally, prepared Car/Alg films were dried in the air at room temperature.

With minor modifications, this procedure was also used to prepare films additionally containing poloxamer or curcumin (besides polysaccharides and plasticizer). During the preparation of films containing polysaccharides and poloxamer (Car/Alg/Pol), a poloxamer 407 aqueous solution was added to the saccharide mixture at the beginning of film preparation. The rest of the procedure was identical to that for Car/Alg films. To prepare films containing curcumin (Car/Alg-Cur and Car/Alg-Pol-Cur), ethanol solution of curcumin (5.0 mL 1.0%, w/v) was added to the mixture (30.0 mL) of starting components (saccharides/ saccharides and poloxamer) after 30 min of stirring. Then, stirring was continued at room temperature for another 30 min, and further work process was identical to that previously described.

### 2.3. Optimization of film composition

To obtain films with the most favorable mechanical properties and high swelling degree, films with different concentrations of glycerol as a plasticizer (25 −80% glycerol by saccharides weight), different total concentrations of saccharides (1.5%, 2.0%, and 3.0% w/w) and different saccharides ratios in the mixture (Car/Alg − 2:8, 4:6, 5:5, 6:4 and 8:2) were prepared and investigated in this study. Also, the optimal

concentration of poloxamer in Car/Alg/Pol films was determined. In the process of preparation of Car/Alg/Pol films, poloxamer solutions of different concentrations (1.5%, 3.0%, 5.0%, 10.0%, 15.0%, w/w) were added. In the second phase of film preparation, the crosslinking time was varied (5, 10, 15, and 20 min). Based on the mechanical properties of the obtained formulations and the swelling degree values, formulations with optimal concentrations of starting components were determined, as well as the optimal crosslinking time, which is used in the further experiment.

### 2.4. Film characterization

#### 2.4.1. FTIR spectroscopy

The prepared films' composition was characterized using FTIR spectroscopy (Perkin Elmer Spectrum Two). The pure starting materials (Car, Alg, Pol, Cur) were also analyzed. All spectrums were recorded in a wavenumbers range of 4000–500 cm$^{-1}$.

#### 2.4.2. Swelling degree

Swelling degree is one of the most important criteria for determining optimal films. Films based on polysaccharides and films based on polysaccharides and poloxamer were used for swelling studies. Parts of the films (2 ×2 cm) of defined mass ($m_0$) were immersed in an appropriate volume of buffer (PBS buffer, pH=7.4) and incubated at 37 °C. The weight of hydrated films ($m_e$) was measured during defined time intervals. Swelling degree (w) was calculated using Eq. 1.

$$w \quad (\%) = \frac{m_e - m_0}{m_0} \times 100\%$$ (1)

All measurements were performed in triplicate.

#### 2.4.3. Scanning electron microscopy (SEM)

The surface morphology of the films was analyzed by scanning electron microscope JOEL JSM IT 300LV, at an accelerating voltage of 20 kV. Images were captured at magnification of 1000 × .

#### 2.4.4. Thermogravimetric analysis (TGA)

Thermal characteristics of prepared films and starting materials were determined using thermogravimetric analysis (instrument TGA701, Leco). The method involved samples heating in a temperature range between 20 °C and 450 °C, at a rate of 10 °C/min in an inert atmosphere. The loss in the sample mass during the analysis is caused by the evaporation of the present water (lower temperatures) and the degradation of film components (higher temperature), resulting in the formation of volatile compounds. The temperatures at which mass changes occur were determined using thermogravimetric analysis.

#### 2.4.5. XRD analysis

To determine the crystalline/amorphous nature of drugs and polymers comprising the films, X-ray diffraction (XRD) analysis of the prepared films was performed. XRD analysis was performed using "RigakuMiniFlex 600" with "D/teX Ultra 250" high-speed detector and copper anode X-ray tube. The measuring conditions were as follows: 3–90° angle range, 0.02° increments, 10°/min recording speed, 40 kV X-ray tube voltage, and 15 mA current.

#### 2.4.6. Determination of encapsulation efficiency

The efficiency of curcumin encapsulation was determined by immersing the films with the incorporated drug in phosphate buffer pH 7.40. After 24 h, aliquots were taken, and the concentration of encapsulated curcumin was determined using UV/Vis spectrophotometry (Perkin Elmer UV/Vis, Lambda 365) at the wavelength of 430 nm. The ratio of spectrophotometrically determined mass of drug and mass of drug added to films during film preparation represents the encapsulation efficiency-EE% (Eq. 2). Measurements were performed in triplicate.

$$EE(\%) = \frac{\text{Spectrophotometrically determined amount of } curcumin}{\text{Added amount of } curcumin} \times 100$$

(2)

### 2.5. In vitro release of curcumin

*In vitro* release of curcumin from the films containing the drug was monitored in conditions simulating wound exudate. The change in the concentration of curcumin released from the optimal films (previously determined optimal concentration of glycerol, saccharides, and poloxamer 407, optimal crosslinking time) was monitored in PBS buffer, pH value 7.4. During the curcumin release assay, 2 × 2 cm films (containing 2.83 mg curcumin) were added to the buffer solution and incubated at 37 °C. From aliquots taken at certain time intervals during 24 h, the concentration of released curcumin was determined spectrophotometrically by measuring the absorbance at 430 nm. Measurements were performed in triplicate.

### 2.6. The kinetics of curcumin release

Based on the results obtained during the *in vitro* release of curcumin, the kinetics indicating the mechanism of curcumin release from films was determined. The release kinetics was analyzed using various mathematical models, which included zero-order kinetics, first-order kinetics, Higuchi and Korsmeyer–Peppas release model (Eqs. 3–6), where $M_t/M_\infty$ is a fraction of released drug at time (t), and k is release constant [45].

Zero order *kinetic* $\quad M_t/M_\infty = kt$ (3)

First order *kinetic* $ln(M_t/M_\infty) = kt$ (4)

Higuchi release model $M_t/M_\infty = kt^{1/2}$ (5)

Korsmeyer − Peppas release *model* $M_t/M_\infty = kt^n$ (6)

A mathematical model that best describes the release of drugs from films can be determined based on the correlation coefficient ($R^2$) value. Also, release exponent *n* can indicate the mechanism of drug release.

### 2.7. Computational details

In order to examine the interaction between curcumin and drug carrier containing κ-carrageenan, calcium-alginate, and poloxamer 407, the structures of isolated molecules were optimised at the B3LYP/def2-SVP level of theory. All optimisations were carried out using Gaussian 09 [46]. Local minima were verified by the calculation of vibrational frequencies. Subsequent optimisations of the complexes were performed with the semiempirical PM6 method, due to a computational cost reduction. Starting from the so-obtained structures SPE calculations were done at the B3LYP/def2-SVP level of theory. All optimisations were done according to the scheme proposed in recent work [47]. The optimisations were done for six positions of two molecular systems, which adopt face-to-face, side-to-side, and perpendicular arrangements. Only the most stable structures were further examined. The first phase (P1) was the optimisation of κ-carrageenan and calcium-alginate. Poloxamer units were added to the complex obtained in P1, and the new complex was also optimised – phase 2 (P2). Curcumin was added to the structures resulted from phase 1 and phase 2, labelled as CP1 and CP2. Incorporation of curcumin into drug carrier, and controlled release of curcumin were examined by the bond dissociation energies (BDE), NBO analysis [48], and AIM analysis [49]. NBO analysis was used as implemented in Gaussian 09 software [41], while AIM analysis was done by Multiwfn [50]. BDE was calculated as the difference between the sum of energies of frozen fragments and the energy of the obtained complex:

$$BDE_{CP1} = (E_{CA} + E_{cur}) - E_{CP1}$$ (7)

$$BDE_{CP2} = (E_{CAP} + E_{cur}) - E_{CP2} \qquad (8)$$

$E_{CA}$ refers to the energy of κ-carrageenan and calcium-alginate, $E_{cur}$ to the energy of curcumin, $E_{CAP}$ is the energy of κ-carrageenan, calcium-alginate and poloxamer 407, while $E_{CP1}$ and $E_{CP2}$ are the energies of the curcumin-phase 1 and curcumin-phase 2 aggregates. These BDE energies can be a measure of the interaction strength between curcumin and the structures resulted from phases 1 and 2. Thereafter, the BDE can answer which drug carrier can be used for controlled release of curcumin. The NBO and AIM analysis can be used to define interactions between the curcumin and these two drug carriers. The NBO analysis were used to examine crucial donor-acceptor interactions between curcumin and drug carriers. Within AIM analysis, the bond critical points (BCP) were investigated to analyze the mechanism of bonding interactions. All total energy values were corrected for the basis set superposition error (BSSE) by the counterpoise method proposed by Boys and Bernardi [51].

### 2.8. Cell viability assay

The study of cell viability (proliferation) in the presence of Car/Alg/Pol-Cur films was determined using a standard MTT test [52].

#### 2.8.1. . Cell culture

A human fetal lung fibroblast cell line (MRC-5) was used to evaluate the cytocompatibility of Car/Alg/Pol-Cur films. The MRC-5 cells were cultured in Dulbecco's modified eagle medium supplemented with 10% fetal bovine serum, 100 U/mL penicillin, 100 μg/mL streptomycin, 2 mM L-glutamine, and 1 mmol/L non-essential amino acids. Cells were cultivated at 37 °C in an atmosphere of 5% $CO_2$ and absolute humidity. The culture medium was completely replaced every 3 days, cell viability was determined using trypan blue staining, and only cell suspensions with viability greater than 95% were used.

#### 2.8.2. . Cell viability assay

A viability study of Car/Alg/Pol and Car/Alg/Pol-Cur films was performed using an MTT assay. Before *in vitro* experiments, the films were cut into cylinders of 9 mm in diameter (curcumin concentration used for fibroblast proliferation study was below 50 ppm [53]). The films were transferred into 96-well plates and irradiated by ultraviolet light for 30 min. The suspensions of MRC-5 cells (5000 cells per well, according to studies [12,13]) were dropped onto the sample surfaces. The control group received the same amount of MRC-5 cells in the blank dishes. The plates were incubated for 24 and 48 h at 37 °C in an atmosphere of 5% $CO_2$ and absolute humidity. Then, MTT solution was added to cell culture and incubated. After incubation, MTT solution was removed, and DMSO was added. Absorbance was measured at 595 nm with a multiplate reader (Zenith 3100, Anthos Labtec Instruments GmbH). Experiments were performed in triplicates and repeated in three independent series.

### 2.9. In vivo wound healing study

The application of prepared films with incorporated curcumin for healing wounds caused by burns was *in vivo* examined. Male Wistar albino rats (6–8 weeks old, mean body weight 200–250 g) were used in the study. One group of animals (n = 3) was exposed to burns and not further treated (control), the second group (n = 3) was treated with Car/Alg/Pol films, and the third (n = 5) with Car/Alg/Pol-Cur films. The process of causing burns to rats was performed according to the protocols of a previously published study [54]. The animals were anesthetized with intraperitoneal ketamine (10 mg/kg of body weight) and xylazine (5 mg/kg of body weight) before causing burns. The backs of healthy rats were shaved using depilatory cream. The burns were caused on the shaved skin area using a red-hot metal plate (dimensions 2 ×2 cm) pressed against the skin for 10 s. The resulting wounds were covered with prepared films (dimensions 2 ×2 cm). The healing process
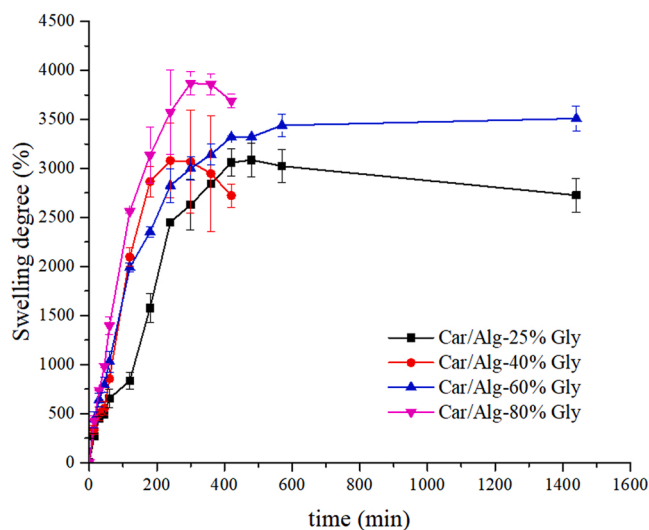


**Fig. 1.** Swelling degree of films with different plasticizer concentration.

was monitored for 7 days, while film samples were replaced on a daily basis. All the animal research studies were approved by the Animal Ethics Committee of the Faculty of Medicine, University of Kragujevac (Ethical Approval Number: 01–6121).

#### 2.9.1. . Histopathological examination

The intensity of heated metal plate caused injury and recovery of burn wound tissue after film treatment were assessed based on the histopathological assessment of both healthy and burned skin. All rats were sacrificed by means of cervical dislocation on day 7 post-burning. The skin was aseptically removed and fixed in 10% buffered formalin fixative overnight. Paraffin wax embedded skin sections (5 μm) were stained with hematoxylin and eosin (H&E), and stained slides were then examined under a light microscope to evaluate the extent of damage. The images were captured with a light microscope (Olympus) equipped with a digital camera.

## 3. Results and discussion

### 3.1. Optimization of films' composition

The optimization process included an analysis of the influence of the total concentration and ratio of polymers on the properties of the obtained films and the effect of plasticizer and poloxamer concentration. Additionally, films obtained after different crosslinking times were compared. During the film optimization process, high-viscosity formulations, non-homogeneous and non-transparent formulations, films with visible mechanical damage or air bubbles after drying, or with undissolved substance on the film surface were excluded from the further experiment. After this preliminary estimation, the swelling degree and stability of the films in the buffered medium were used as criteria for further analysis of film quality. Finally, films with optimal characteristics were used for drug incorporation.

Studies have found [15,55] that added plasticizer has a favorable effect on the mechanical properties of the films − the films are more flexible, have no visible deformations, and can be easily separated from the Petri dish surface. In addition, with the increase in plasticizer concentration, the film thickness can also increase due to the formation of a better polymer network, leading to easier film separation and improved elasticity [56]. Also, thicker films show a better tendency to swell. In this paper, films prepared with lower glycerol concentrations (25% and 40%) could not be easily separated from Petri dishes and had pronounced brittleness. Films with 60% and 80% glycerol concentrations were similar in thickness and mechanical properties. Fig. 1 shows the
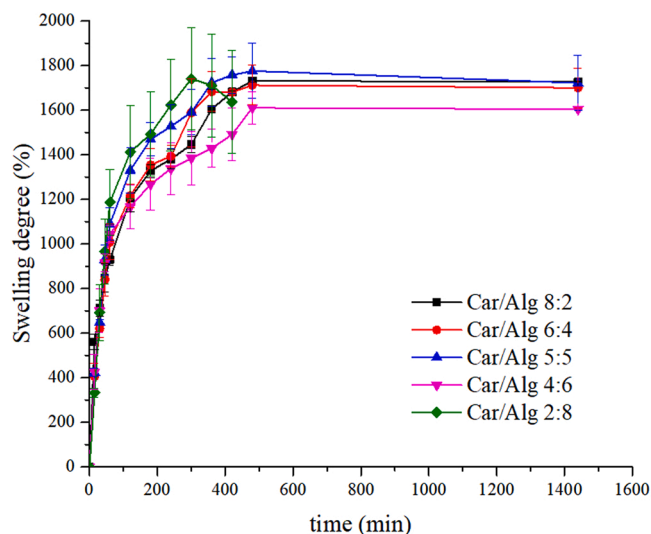
**Fig. 2.** Swelling degree of films in different ratio κ-carrageenan/alginate.



**Fig. 3.** Swelling degree of films obtained after different crosslinking time.

time dependence of the swelling degree of films with different glycerol concentrations.

Fig. 1 also shows that all analyzed films have high swelling degree values in the first hours after immersion in the buffer. However, after 5 h, the swelling degree of films with 80% and 40% glycerol started to decrease (due to dissolution in the buffer), and after 7 h, the films were deformed. For this reason, the swelling degree was not further monitored. Films with 25% and 60% glycerol kept shape for 24 h, but after 8 h, the swelling degree of the 25% glycerol film began to decrease due to partial dissolution in the buffer. The 60% glycerol film showed a high swelling degree constantly growing for 24 h, indicating the good ability for controlled 24-hour release, so this plasticizer concentration was used in the further experiment.

As part of film composition optimization, the total concentration of saccharides in the mixture was also varied (1.5%, 2.0%, and 3.0%). Films obtained using saccharides with a total concentration of 3.0% had undesirable physical characteristics, such as high brittleness (Fig. S1A, Supplementary material). Films with 1.5% and 2.0% polymer concentrations were prepared with different ratios of components (Car/Alg 2:8, 4:6, 5:5, 6:4, and 8:2) and had no visible mechanical defects. However, films with a lower saccharide concentration (1.5%) were thinner and more sensitive to handling, so 2.0% saccharide concentration was used in the further experiment. After examining the obtained carriers with different carrageenan/alginate ratios, films with higher alginate content were found to be more difficult to separate from the Petri dish surface due to stronger adhesive forces. Additionally, films were thinner, with a greater tendency to tear. The swelling degree (Fig. 2) was also examined as a criterion for determining the optimal saccharide ratio.

The obtained results show that higher alginate content in films contributes to higher solubility rates of films in the buffer. In comparison, films with higher carrageenan content were stable in the buffer for 24 h, and there was no change in film shape during the experiment. Considering all the above discussions, the film with Car/Alg ratio of 8:2 was used in the further experiment (this film had the highest swelling degree that had not decreased over time).

Different studies [15,55] have investigated the incorporation and release of hydrophobic drugs from films based on polysaccharides and poloxamer 407. Added poloxamer, as a surfactant, was found to increase the degree of encapsulation of poorly soluble drugs [15,55,57,58]. Curcumin, the drug analyzed in this study, belongs to highly hydrophobic compounds, so adding poloxamer to polysaccharide mixtures should improve curcumin encapsulation and stability into films [59,60]. In this paper, different concentrations of poloxamer (1.5%, 3.0%, 5.0%, 10.0%, 15.0%, w/w) were examined. Films with a poloxamer
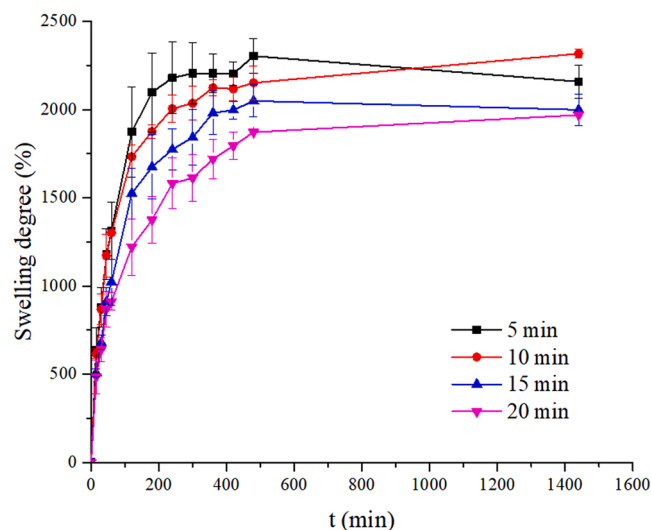
concentration greater than 5.0% had many residual air bubbles that could not be removed using an ultrasonic bath and remained in the films even after drying (Fig. S1B, Supplementary material). The presence of bubbles negatively affects the mechanical properties of films and their efficiency during drug release. In addition, the prepared films were less transparent due to the poloxamer crystallization [55]. For this reason, films with poloxamer concentrations above 5.0% were not used in the further experiment. After the addition of curcumin, it was found that films containing poloxamer concentrations lower than 5.0% could not completely dissolve curcumin because it remained on the film surface (Fig. S1C, Supplementary material). Consequently, the experiment was continued with a poloxamer concentration of 5.0%.

Films containing alginate as a constituent component can be further crosslinked by film immersion in a solution containing a higher concentration of calcium chloride and plasticizer than that used in film preparation. In this way, the stability of the films in solution will increase [11]. Calcium ion binds to groups from guluronic acid in alginate and enables the formation of a network of this biopolymer. Due to the higher water content, better elasticity, permeability, and the ability to form a moisture environment, formulations containing alginate can be used in the wound healing process [8,10,61]. A higher concentration of plasticizer in the crosslinking solution allows the films to retain flexibility even after drying [55,62]. In this paper, different crosslinking times, in the interval 5 − 20 min, were examined.

All fully crosslinked films had satisfactory mechanical stability, flexibility and showed no shape deformation during the crosslinking process. The swelling degree of the Car/Alg/Pol films (obtained after different crosslinking times) as one of the basic criteria for determining optimal crosslinking time is shown in Fig. 3.

Considering that the films kept their initial shape during the swelling experiment (24 h), it can be concluded that the crosslinking process contributed to the stability improvement of the formulations. Also, it can be seen that a shorter crosslinking time (5 min) leads to a higher swelling degree value, but after 12 h, the swelling degree begins to decrease due to partial dissolution of the films. The swelling degree of films with crosslinking times of 15 and 20 min has not changed after 12 h, while for films with a crosslinking time of 10 min, there was a constant increase over 24 h. Accordingly, crosslinking time of 10 min was used in the further experiment.

### 3.1.1. . Curcumin encapsulation

Curcumin has been successfully incorporated into polysaccharide-based carriers and carriers containing both polysaccharides and poloxamer (Fig. S1D, Supplementary material). The encapsulation efficiency
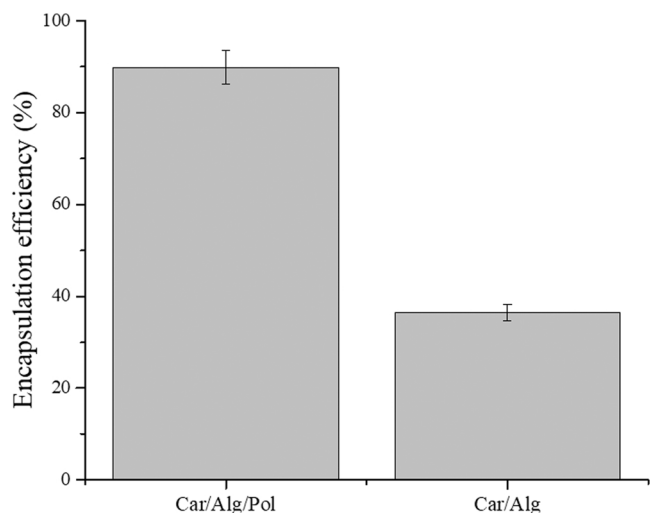
**Fig. 4.** Encapsulation efficiency of curcumin.

**Table 1**
Characteristics of films (n = 5).

| Film | Film weight $(mg/cm^2)$ | Film thickness $(\mu m)$ | Mass of curcumin (mg/$cm^2$ of film) |
|---|---|---|---|
| Car/Alg | $10.55 \pm 0.45$ | $97.59 \pm 1.94$ | / |
| Car/Alg/Pol | $12.21 \pm 0.65$ | $104.27 \pm 3.35$ | / |
| Car/Alg/Pol-Cur | $13.03 \pm 0.74$ | $117.11 \pm 3.66$ | $0.708 \pm 0.026$ |

of curcumin in Car/Alg-Cur and Car/Alg/Pol-Cur films was also determined (Fig. 4).

Based on the obtained results, it can be noticed that encapsulation efficiency is significantly higher for films containing poloxamer as a surfactant. Also, the percentage of curcumin encapsulation (89.85 $\pm$ 3.67)% obtained for Car/Alg/Pol-Cur films indicates that no major losses occurred during the film preparation. Polysaccharide- and poloxamer-based carriers easily interacted with the added drug, forming a single, homogeneous film that enhances curcumin bioavailability.

### 3.2. Film characterization

#### 3.2.1. Basic characteristics of films

Table 1 shows the average masses and thickness of the obtained films, as well as the mass of incorporated curcumin in films of optimal composition. It can be concluded from the obtained results that films of the same composition show uniformity in terms of both mass and thickness.

#### 3.2.2. FTIR spectroscopy

The FTIR spectra of the starting components carrageenan, alginate, poloxamer, and curcumin, as well as of Car/Alg, Car/Alg/Pol, and Car/Alg/Pol-Cur films are shown in Fig. 5A and B. In carrageenan and alginate spectra, wide absorption bands in 3400–3200 $cm^{-1}$ and 3000 − 2840 $cm^{-1}$ wavelength ranges can be observed, originating from the valence vibration of the O−H bond and the C−H bond, respectively. The absorption band at 1224 $cm^{-1}$ is characteristic of the carrageenan spectrum, and it is caused by the valence vibrations of S=O bonds from the present sulfate groups. In the spectrum of alginate, characteristic bands at 1598 and 1407 $cm^{-1}$ can be observed resulting from asymmetric and symmetric vibrations of the carboxylate anion, respectively. In the poloxamer spectrum, a band at 2881 $cm^{-1}$ (the result of valence vibrations of C−H bonds) is observed, but also a very intense band at 1098 $cm^{-1}$ (due to valence vibrations of C−O bonds) which is characteristic of polyethylene oxide. In the curcumin spectrum, a sharp band at 3508 $cm^{-1}$ is attributed to vibration of phenolic O−H groups. Also, a band at 1628 $cm^{-1}$ can be noticed, resulting from C=O stretching vibration.

In the spectra of Car/Alg, Car/Alg/Pol, and Car/Alg/Pol-Cur films, wide absorption bands can be noticed in the range 3500 − 3000 $cm^{-1}$, resulting from valence vibrations of the O−H bonds presented in saccharides. Also, valence vibrations of C−H bonds that occur in the range of 3000 − 2840 $cm^{-1}$ can be observed. The IR spectrum of carrageenan-alginate film contains all the vibrations of the groups that are characteristic of both carrageenan (sulfate group) and alginate (carboxylate anion). Therefore, it can be concluded that a unique carrageenan-alginate aggregate was formed. As a consequence of the polysaccharides interaction, there was a slight shift in the wavenumber values (1224→1242, 1406→1417 and 1598→1615 $cm^{-1}$) which corresponds to the characteristic vibrations of carrageenan and alginate. On the other hand, when poloxamer is added to the carrageenan-alginate mixture, its presence in Car/Alg/Pol film can be confirmed by a very intense band that occurs at about 1035 $cm^{-1}$ and corresponds to the vibration of the C−O bond, which is characteristic of the poloxamer. Adding curcumin (Car/Alg/Pol-Cur spectrum) leads to a slight shift of bands which corresponds to vibration of alginate carboxylate anion (1417→1455 and 1615→1624 $cm^{-1}$) that may be a consequence of the vibration of carbonyl group presented in curcumin.

#### 3.2.3. Scanning electron microscopy (SEM)

The study of morphology and the surface characteristics of the Car/Alg, Car/Alg/Pol, Car/Alg-Cur, and Car/Alg/Pol-Cur films was done using scanning electron microscopy (Fig. 6).
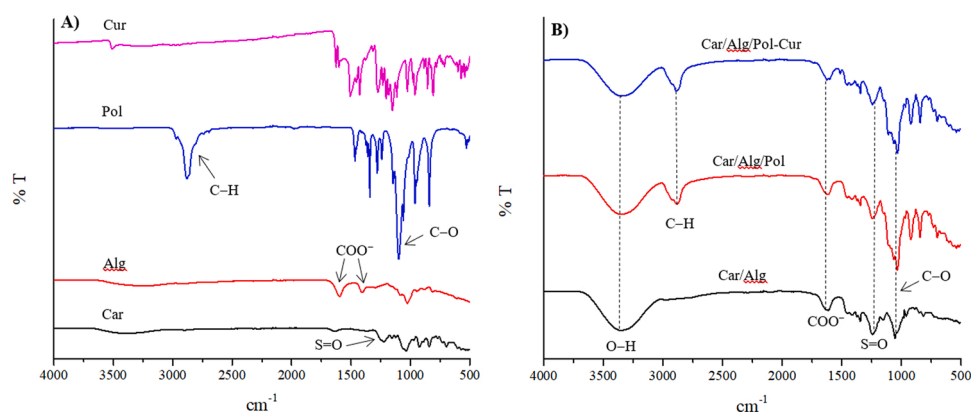


**Fig. 5.** A) FTIR spectra of starting components – carrageenan, alginate, poloxamer 407 and curcumin, B) FTIR spectra of prepared films – Car/Alg, Car/Alg/Pol and Car/Alg/Pol-Cur.
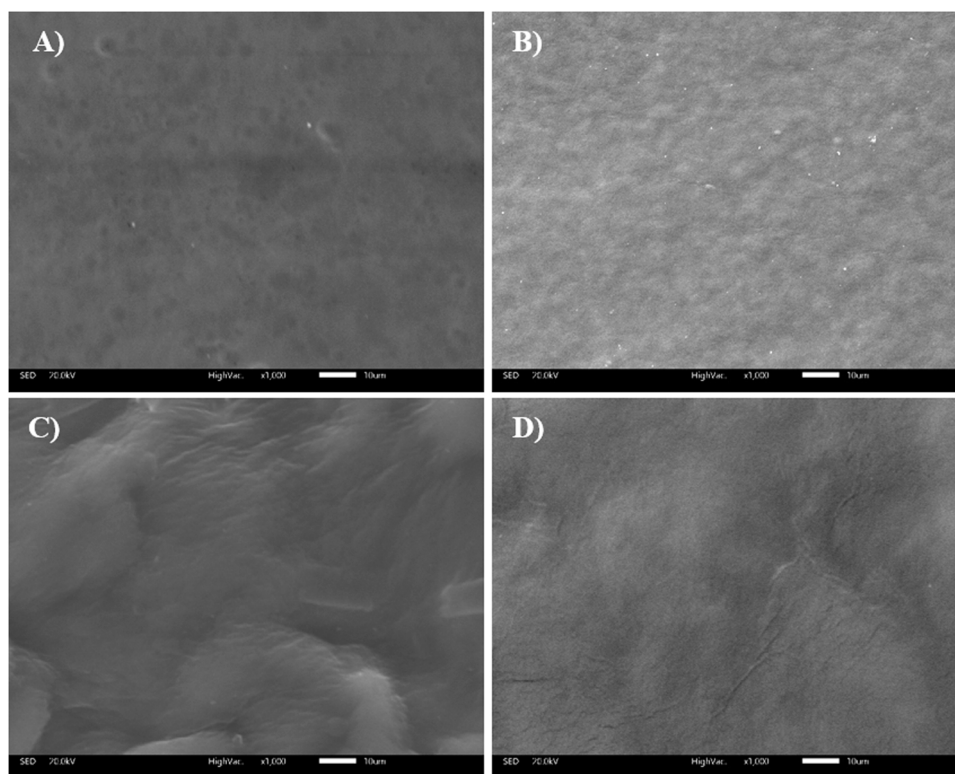
**Fig. 6.** SEM images (×1000) A) Car/Alg, B) Car/Alg-Pol, C) Car/Alg-Cur, D) Car/Alg/Pol-Cur films.
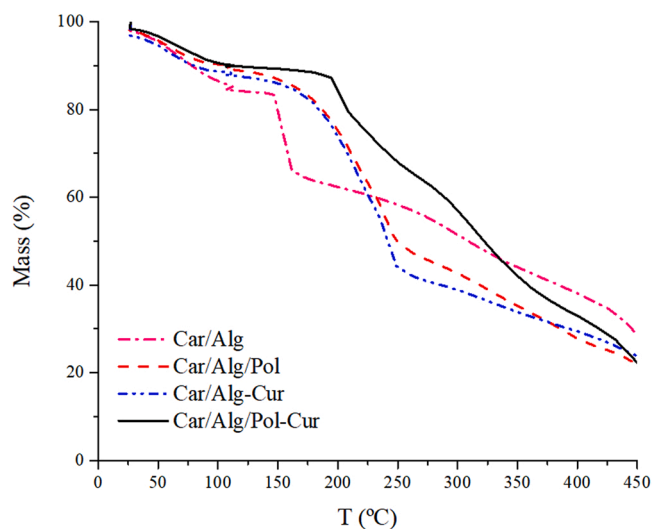


**Fig. 7.** Thermogravimetric curves of Car/Alg, Car/Alg/Pol, Car/Alg-Cur and Car/Alg/Pol-Cur films.

Fig. 6 shows that the film surface is smooth and has no visible pores, indicating film homogeneity. The Car/Alg and Car/Alg/Pol films had a very smooth and uniform surface. Traces of undissolved poloxamer could be seen on the Car/Alg/Pol film surface (Fig. 6B). In the SEM image corresponding to the Car/Alg-Cur film (Fig. 6C), it can be seen that the curcumin is present on the film surface in crystalline form. Adding poloxamer leads to better curcumin incorporation within the film and the formation of a more uniformed film surface (Fig. 6D).

*3.2.4. Thermogravimetric analysis*

The thermal stability of the films was studied using thermogravimetric analysis. Fig. 7 shows the thermogravimetric curves

corresponding to Car/Alg, Car/Alg/Pol, Car/Alg-Cur, and Car/Alg/Pol-Cur films.

The initial mass loss, which occurs at temperatures below 100 ºC, is caused by the evaporation of the present, weakly bound water that remained after drying in the process of film preparation or water absorbed by the films from the air. The loss of mass that occurs at a temperature of about 150 ºC (Car/Alg) and continues up to 190 ºC is the result of glycerol evaporation, which is present in films as a plasticizer [63]. As shown in Fig. 7, adding poloxamer and curcumin leads to an increase in thermal stability, so the described loss of mass due to glycerol evaporation takes place at higher temperatures, in the range of 180–240 ºC. At temperatures above 200 ºC (Car/Alg), as well as 250 ºC (Car/-Alg/Pol, Car/Alg-Cur, and Car/Alg/Pol-Cur), there is a loss in mass due to degradation of the initial components, carrageenan and alginate [11, 64]. Based on the presented thermogravimetric curves, it can be concluded that adding curcumin (Car/Alg-Cur) and poloxamer (Car/-Alg/Pol) similarly affects the thermal stability of the analyzed films. However, films that include both poloxamer and curcumin (Car/-Alg/Pol-Cur) show even greater stability compared to the above films.

*3.2.5. XRD analysis*

The physical form (crystalline or amorphous) of the films and the substances forming the films was determined using X-ray diffraction. Fig. 8A and B show the diffractograms obtained for the basic components and for the prepared films.

The obtained results indicate that the formation of films leads to a decrease in crystallinity degree, which can be explained by the interactions between the starting components. It can be noticed that the basic components (primarily carrageenan and alginate) have a low degree of crystallinity (Fig. 8A). However, the formed carriers (Car/Alg and Car/Alg/Pol) existed only in amorphous form (Fig. 8A). Two signals, which appeared at 40º and 45º, do not relate to the analyzed films but are the result of the collision of X-rays on the aluminum carrier of the XRD device during recording, as a consequence of small film thickness, $97 - 135$ μm. The results indicated that curcumin, as a pure substance,
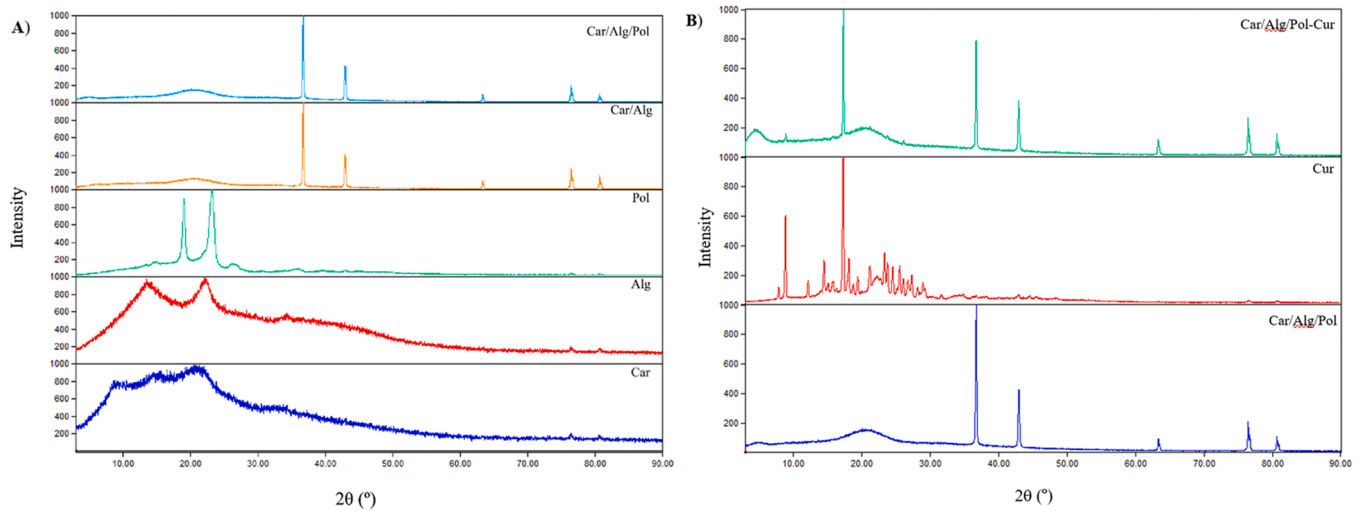
**Fig. 8.** A) XRD patterns of carrageenan, alginate, poloxamer, Car/Alg and Car/Alg/Pol films, B) XRD patterns of curcumin, Car/Alg/Pol and Car/Alg/Pol-Cur films.
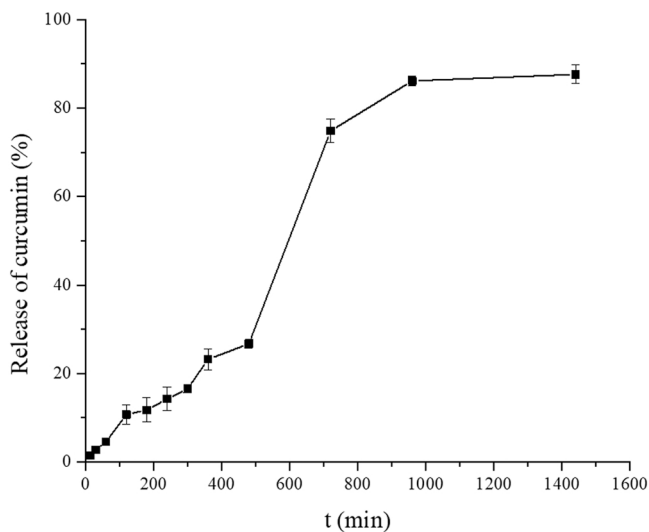


**Fig. 9.** *In vitro* release of curcumin from film Car/Alg/Pol-Cur (n = 3).

was presented only in crystalline form (Fig. 8B). By observing the Car/Alg/Pol-Cur film diffractogram, it can be concluded that drug incorporation into the carrier reduced the curcumin crystallinity degree (Fig. 8B).

### 3.3. In vitro release study

Unlike films containing poloxamer, the results of the studies of *in vitro* release of curcumin from Car/Alg-Cur films indicated that there was no significant drug release from the carrier even after a period of 24 h (figure not shown). *In vitro* curcumin release from Car/Alg/Pol-Cur film, monitored for 24 h, is shown in Fig. 9. By observing the process of curcumin release, it can be concluded that the carrier composition significantly improved the bioavailability of curcumin. In addition, the use of analyzed carriers leads to the gradual release of curcumin over

time, which can prolong the curcumin effect.

Fig. 9 points out that curcumin had been slowly released in the first 8 h. In the period from 8 to 12 h, there was a strong increase in the percentage of release, which finally stabilized in the period from 16 to 24 h, with a maximum value of $(87.64 \pm 2.40)$% (for the encapsulated curcumin mass). Similar results of curcumin release were obtained in the study [65] that analyzed polycaprolactone and chitosan-based films. However, if the results obtained in our paper are compared with those of the study [66] in which curcumin efficiency and bioavailability were improved by its complexation with the cyclodextrin derivative within the saccharin film, it can be concluded that better results were obtained in our paper. The percentage of curcumin release from the complex with cyclodextrin in the first 24 h is about 50% [66], which is significantly less compared to the percentage of release achieved in our research (87.64%). Further comparison of the obtained results with the results of other studies [67] reveals the advantages of carrageenan, alginate, and poloxamer-based films. The release percentage in the first 24 h is only 8.4%. After 5 days, it reaches a maximum value of 40% for the encapsulated weight of 2.65 mg, achieved in the study [67], while the results of release percentage of 87.64% (in 24 h) achieved in our study refer to an encapsulated curcumin weight of 2.85 mg.

From the obtained results, by monitoring the *in vitro* release process, it can be concluded that the use of carrageenan, alginate, and poloxamer-based films achieved continuous drug release over time and maintained film stability. Since curcumin is known to have a positive effect on the proliferation phase during wound healing, a further experiment was dedicated to examining the effect of prepared films on cell viability. Also, the ability of the prepared curcumin-containing films to enhance wound healing was studied *in vivo*.

### 3.4. Curcumin release kinetics

To study the mechanism of curcumin release from films, equations corresponding to zero-order kinetics, first-order kinetics, and the Higuchi and Korsmeyer-Peppas release model were applied to the results obtained by monitoring *in vitro* curcumin release. The values of the correlation coefficients achieved by fitting the results in accordance

**Table 2**
Values of correlation coefficients, release rate constants and release exponent.

| Zero order kinetics | | First order kinetics | | Higuchi model | | Korsmeyer−Peppas model | | |
|---|---|---|---|---|---|---|---|---|
| $k_O$ | $R^2$ | $k_I$ | $R^2$ | $k_H$ | $R^2$ | $k_{KP}$ | $n$ | $R^2$ |
| 0.0492 | 0.9005 | 0.1578 | 0.7421 | 0.2605 | 0.8756 | 0.0655 | 0.9124 | 0.9063 |
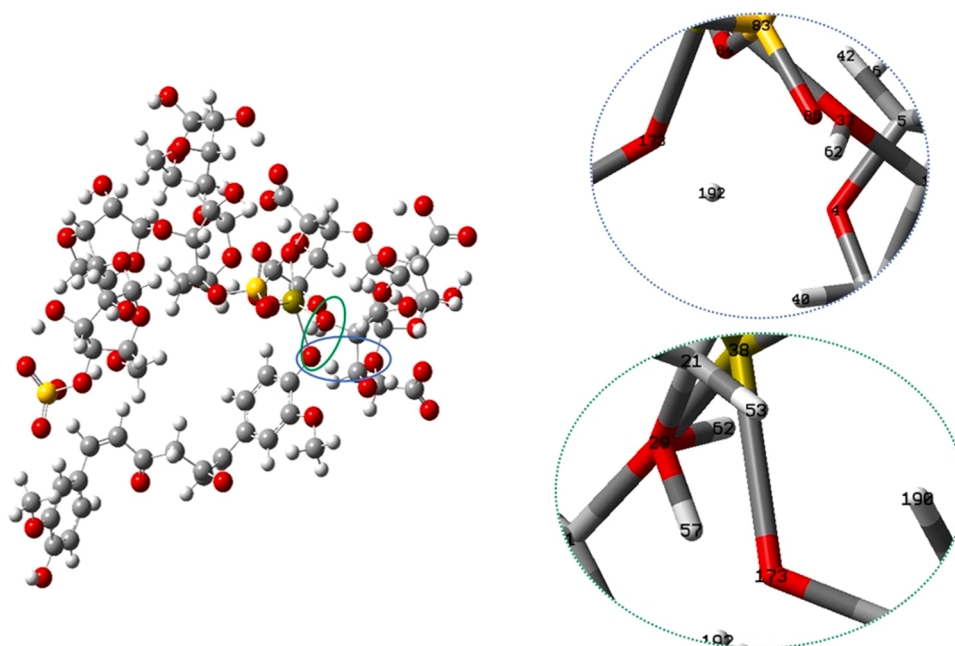
**Fig. 10.** Optimised structure of curcumin with phase 1 - κ-carrageenan and calcium-alginate with established hydrogen bonds.

with the equations corresponding to the models, are shown in Table 2. Also, the values of the release rate constants are shown, as well as the $n$ value in the Korsmeyer−Peppas model.

The correlation coefficient value indicated that the release of curcumin from the Car/Alg/Pol-Cur film was best described by zero-order kinetics. Zero-order kinetics are characteristic of transdermally administered formulations, which are not degradable and do not change carrier surface during release, allowing gradual drug release over time [45]. The Korsmeyer−Peppas model is significant for predicting the drug release mechanism and is mainly used to determine the parameter that has the greatest impact on the release rate (polymer swelling, diffusion of incorporated substance, polymer degradation) [45]. The obtained value for the release exponent $n$ which is 0.5 in the study of thin films, or 0.43 for spherical carriers, directly indicates the release controlled by drug diffusion. In contrast, the value of n = 1, and n = 0.93 for spherical particles indicate that drug release occurs primarily due to polymer swelling [45]. If the $n$ values differ from the above, then the release mechanism is influenced by several factors. In general, values of the release exponent below 0.5 correspond to diffusion controlled by Fick's law, above 0.5 correspond to diffusion that does not obey this law (release caused by polymer erosion), and values above 1 correspond to the case of "super- transport" [45]. The value of n = 0.91 (which is close to n = 1) obtained in the study of curcumin release from the Car/Alg/Pol-Cur formulation indicated that the release mechanism was mainly dependent on polymer swelling, which is characteristic of zero-order kinetics. This result is in accordance with the highest correlation coefficient obtained for zero-order kinetics during the curcumin release study.

### 3.5. Theoretical study of component interaction in developed films

The experimental procedure given above was further computationally rationalized. Using the optimised structures of all employed molecules (Fig. S2, Supplementary material), the interaction between them was computationally quantified and compared with the one experimentally measured. In phase 1, optimised structures of κ-carrageenan and calcium-alginate are approximated to each other by different positions (face-to-face, side-to-side, and perpendicularly), as suggested in recent work [47]. The energies of thus obtained structures were recalculated at the B3LYP/def2-SVP level of theory. The most stable structure
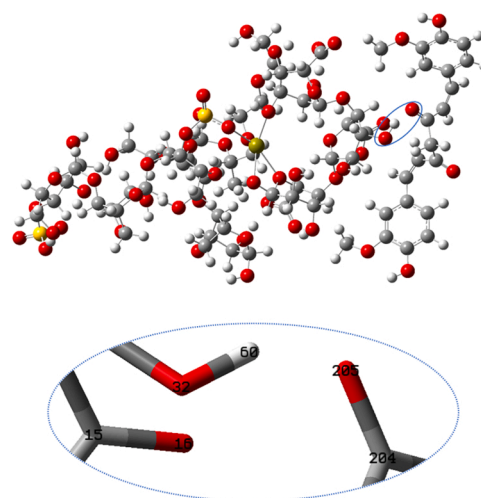


**Fig. 11.** Optimised structure of curcumin with phase 2 - κ-carrageenan, calcium-alginate and poloxamer 407.

was obtained when these two molecules were placed perpendicularly (Table S1, Supplementary material). Interaction between κ-carrageenan and calcium-alginate is facilitated by the presence of calcium-ion due to electrostatic interaction between calcium-ion and sulfate-anion in κ-carrageenan. Apart from this electrostatic interaction, there are two significant hydrogen bonds between O28-H56-O79 and O26-H122-O72 (Fig. S3, Supplementary material).

In the next step, phase 2, poloxamer units were added to thus obtained structure using the same arrangements. In order to provide as realistic as possible model of experimental conditions, poloxamer was introduced as a polymer of three ethylene-oxide and two propylene-oxide units, as shown in Fig S2C (Supplementary material). The most stable structure was obtained when poloxamer was added face to face to the phase 1 aggregate (Fig. S4 and Table S2, Supplementary material). The phase 2 form is stabilised by ion-dipole interactions between Ca38 and O160 and hydrogen bonding between O111-H147-O189 and O110-H190-O189. In this way, two drug carriers were formed, labelled as

**Table 3**
BDE and calculated AIM parameters for studied aggregates.

| | BDE (kcal mol$^{-1}$) | observed bond | $\rho_{BCP}$ | $\nabla^2_{\rho_{BCP}}$ | H (r)$\times 10^{-3}$ | $|V (r)|/2$ | $191{,}4 \times \rho_{bcp} - 1{,}78$ |
|---|---|---|---|---|---|---|---|
| CP1 | 35.14 | O4-H192-O173 | 0.0360 | 0.1011 | -0.1491 | 5.11 | -8.03 |
| | | O29-H57-O173 | 0.0313 | 0.1300 | 1.6695 | 4.21 | -9.15 |
| | | Ca38-O173 | 0.0250 | 0.1234 | 4.0489 | / | -7.14 |
| CP2 | 16.56 | O205-H60-O32 | 0.0398 | 0.1299 | 0.3625 | 5.83 | -9.97 |
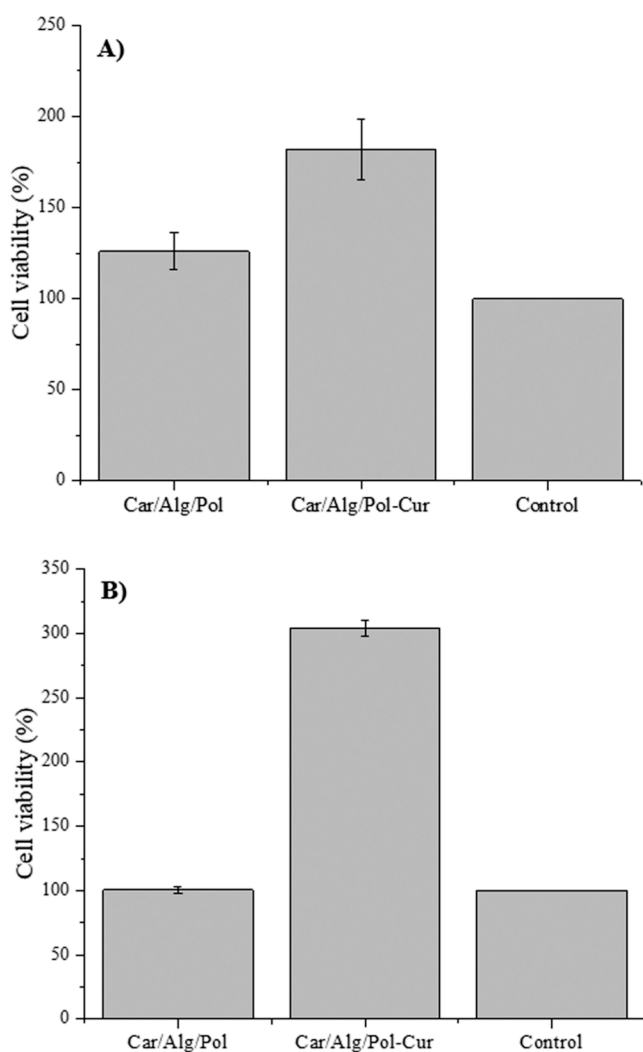


**Fig. 12.** Influence of Car/Alg/Pol and Car/Alg/Pol-Cur films on MRC-5 cell viability after.
A) 24 h i B) 48 h.

phase 1 − κ-carrageenan and calcium-alginate and phase 2 − κ-carrageenan, calcium-alginate, and poloxamer 407.

The next step was to elucidate curcumin interactions with these two drug carriers. When curcumin is approximated to the phase 1 structure, the best orientation is side-to-side (Table S3, Supplementary material). This complex is stabilized by interactions of phenol group in curcumin and phase 1 (Fig. 10). Besides ion-dipole interactions between calcium and oxygen in the phenolic group of curcumin, there are two important hydrogen bonds between the phenolic group in curcumin and calcium-alginate, precisely, O4-H192-O173 and O29-H57-O173. These interactions were further examined within NBO and AIM analysis.

On the other hand, the most stable arrangement of curcumin with the phase 2 form is perpendicular, as shown in Fig. 11 and Table S4 (Supplementary material). This aggregate is stabilized only by one hydrogen

bond between O205 in curcumin and O32-H60 in the phase 2 structure. This means that phase 2 aggregate can be a better drug carrier because the interaction between curcumin and the phase 2 structure is weaker than with phase 1, so curcumin can be easily released, which is in accordance with the BDE values (Table 3). To release curcumin from the curcumin-phase 1 aggregate, 35.14 kcal mol$^{-1}$ is requisite, while releasing curcumin from phase 2 complex requires almost twice less, only 16.56 kcal mol$^{-1}$. These can be further rationalized by employing NBO and AIM methods.

AIM parameters calculated at BCPs are collected in Table 3.

In this case, the value and sign of the electron density ($\rho$BCP) and the electron density Laplacian ($\nabla^2_{\rho_{BCP}}$) can be used as indicators of the nature of bonding between two atoms. If the electron density in BCP has a value less than 0.10 a.u., interaction is weak, such as ionic, van der Waals, hydrogen bonding. All observed interactions in this paper are weak by the electron density. These interactions can be further elucidated by energy density values (H(r)). A negative value for O4-H192-O173 bond indicates strong interaction, but also, in other cases, small hydrogen bonds and van der Waals ion-dipole interaction, such as between calcium and oxygen. Hydrogen bonding can be further examined using formulas proposed in works by Espinosa et al. [68], as well as Karaush *et al.* [69] and Afonin et al. [70]. These results are also given in Table 3. Both formulas give the same prediction - curcumin has a stronger interaction with phase 1-structure than with phase 2-structure, making the phase 2 form a better drug carrier.

NBO analysis can be used to confirm examined interactions. For example, in CP1 complex, oxygen in calcium-alginate, O4, is a donor of electronic pair to the antibonding orbital of the phenolic group (O173-H192) in curcumin. O173 can act as a donor and calcium-ion as an acceptor in this weaker interaction. This phenolic group in curcumin has a significant role in examined interactions. On the other hand, there is hydrogen bonding between O205 in curcumin and H60-O32 in phase 2. AIM and NBO analyses go in line with predictions of possible interactions between curcumin and two examined drug carriers.

### 3.6. Cell viability assay and in vivo wound healing study

#### 3.6.1. . *Cell viability assay*

Influence of Car/Alg/Pol and Car/Alg/Pol-Cur films on the viability of MRC-5 cell lines were examined by MTT test after cell cultivation for 24 and 48 h (Fig. 12).

The obtained results indicate that the film Car/Alg/Pol has no effect on the healing process because the percentage of tested cells viability is the same as in the control cells. However, cell viability was significantly higher in the presence of films containing curcumin during the incubation period of 24 and 48 h. From the obtained results, it can be concluded that the increase in cell viability is due to the presence of curcumin in the films. Based on the percentage of viable cells (Fig. 12), it can also be concluded that curcumin-containing films may have potential application in the wound healing process. The obtained positive results of *in vitro* analysis have directed further research in this paper. Additionally, it was developed that alginate-contained hydrogel dressings show good bioadhesive properties on human tissue [27–29]. Accordingly, the prepared films were tested as formulations potentially applicable in wound healing of the rats' skin.
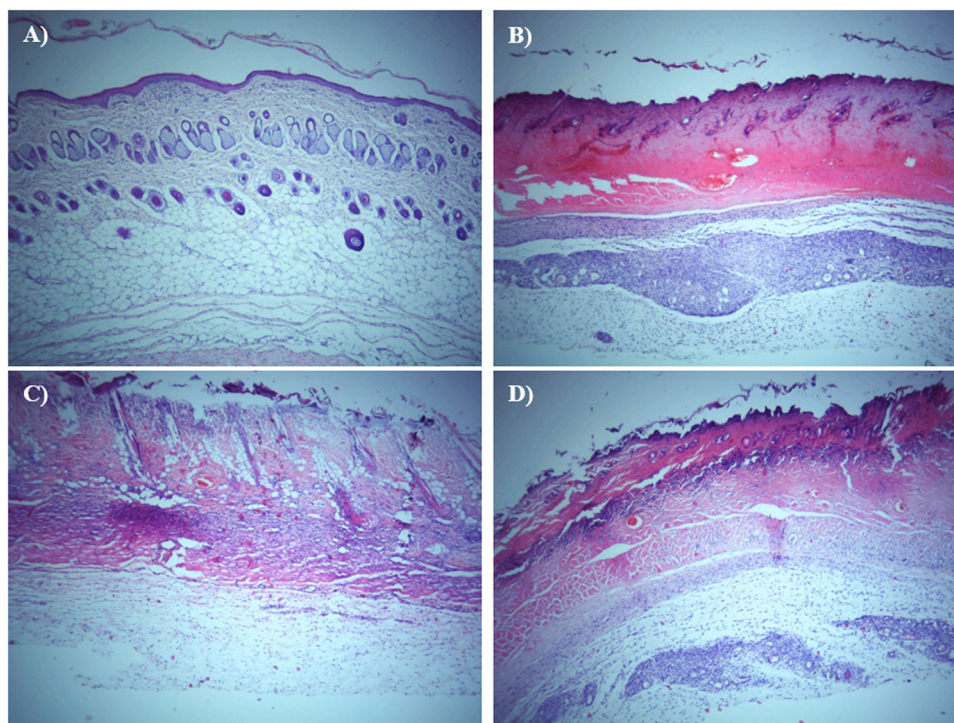
**Fig. 13.** Histopathological observation of H&E stained skin sections (200 ×) of A) healthy skin, B) burned skin, C) burned skin treated with Car/Alg/Pol film, and D) burned skin treated with Car/Alg/Pol-Cur film.

### 3.6.2. . Histopathological analysis

Wound healing, as a complex process, includes inflammation response, new tissue formation, and tissue remodelling. To study the therapeutic potential and effectiveness of prepared films in wound healing process, male Wistar albino rats (aged 6–8 weeks, average body weight 200–250 g) were used for *in vivo* research. During the research, no infection on the caused wounds, no bleeding of the granulation tissue, or the appearance of sepsis was observed. After causing burns, films application for seven days, and rats sacrificing, the upper layer of the wound was surgically removed and subjected to histological studies. Photomicrographs of healthy skin (before burn), burned skin (after burn), as well as treated skin stained with hematoxylin and eosin are presented in Fig. 13.

Histological assessment of healthy skin indicated that the structure of the thin skin section was normal with intact epithelial layers, sebaceous glands and intact hair follicles (Fig. 13A). This Figure also shows that thin skin was formed of the thin epidermis and thick dermis. Light microscopic examination of burned skin sections of adult male albino rats showed inflammatory changes compared to normal skin (Fig. 13A and B). Burned skin segment demonstrated signs of complete destruction of superficial skin layers, coagulation, infiltration of fibroblasts and polymorphonuclear cells, as well as collagen (Fig. 13B). To assess the degree of skin regeneration, histopathological analysis was performed on the 7th day after treatment (13 C and 13D). In the group treated with Car/Alg/Pol film, there was inflammation in skin tissue with edematous fluid collection in the dermis region, as depicted in Fig. 13C. Photomicrographs indicated that animals treated with Car/Alg/Pol-Cur film (Fig. 13D) showed signs of increased regeneration in the epidermal region in the presence of growing fibroblasts in the granulation tissue. Mild infiltration of neutrophils and hair follicles were also evident (Fig. 13D). Histopathological findings clearly indicated early signs of wound healing after Car/Alg/Pol-Cur film application. The *in vivo* study results are in accordance with the results obtained by cell viability assay in the presence of films. The film containing curcumin had the greatest potential for application in the wound healing process because of its positive effect on the proliferation phase thanks to curcumin.

### 4. Conclusion

Biocompatible polymer-based hydrogels, in film form, have great potential for use in medicine as transdermal systems for skin wounds treatment. In this study, films based on crosslinked polysaccharides, κ-carrageenan and alginate, were prepared. As poloxamer 407 is known to increase hydrophobic drug solubility and encapsulation, this synthetic polymer was also added to the carriers. Different ratios of polysaccharides, different concentration of poloxamer, and glycerol as plasticizer, and different crosslinking times were examined to obtain carriers with optimal properties. The films with optimal properties were obtained using carrageenan and alginate in a ratio of 8:2 and 5.0% poloxamer concentration.

Curcumin, as the drug model, has been incorporated into optimized films with 89.85% encapsulation efficiency. Addition of poloxamer lead to increase curcumin concentration into the optimized films (without poloxamer, curcumin encapsulation efficiency was 36.52%). Computational analysis based on theoretical models showed that the carbonyl group of curcumin establishes a hydrogen bond with the alginate hydroxyl group, which further allows curcumin incorporation into prepared films.

The film characterization indicated that films have a smooth and homogeneous surface; the results of X-ray diffraction showed that curcumin incorporation into films reduces its crystallinity degree. *In vitro* curcumin release was monitored for 24 h, and the results showed that curcumin bioavailability was significantly improved using carrageenan, alginate, and poloxamer-based carriers, with cumulative controlled curcumin release over time (87.64%). From the drug release kinetics results, it was concluded that the polymer swelling degree has the greatest influence on the curcumin release. In addition, it was found that the films are not cytotoxic and that curcumin-containing films can increase cell viability and thus have a beneficial effect on cell proliferation, which is one of the wound healing phases. Finally, considering the *in vivo* study results, it can be concluded that the films based on carrageenan, alginate, poloxamer, and curcumin could have a great potential for healing wounds caused by burns.

## CRediT authorship contribution statement

**Katarina Postolović**: Conceptualization, Methodology, Investigation, Writing – original draft preparation. **Biljana Ljujić**: Investigation, Resources. **Marina Miletić Kovačević**: Investigation, Resources. **Slađana Đorđević**: Formal analysis. **Sandra Nikolić**: Investigation, Resources. **Suzana Živanović**: Resources. **Zorka Stanić**: Conceptualization, Methodology, Writing – review & editing, Supervision.

## Declaration of Competing Interest

The authors declare that they have no known competing financial interests or personal relationships that could have appeared to influence the work reported in this paper.

## Acknowledgments

## Appendix A. Supporting information

Supplementary data associated with this article can be found in the online version at doi:10.1016/j.mtcomm.2022.103528.

## References

[1] J.S. Boateng, K.H. Matthews, H.N.E. Stevens, G.M. Eccleston, Wound healing dressings and drug delivery systems: a review, J. Pharm. Sci. 97 (2008) 2892–2923, https://doi.org/10.1002/jps.21210.

[2] G.S. Schultz, Molecular Regulation of Wound Healing, in: R.A. Bryant (Ed.), Acute and Chronic Wounds: Nursing Management, second ed.,, WB Saunders, St. Louis, 1999, pp. 413–429.

[3] P Martin, Wound healing – aiming for perfect skin regeneration, Science 276 (1997) 75–81, https://doi.org/10.1126/science.276.5309.75.

[4] I.R. Sweeney, M. Miraftab, G. Collyer, A critical review of modern and emerging absorbent dressings used to treat exuding wounds, Int. Wound J. 9 (2012) 601–612, https://doi.org/10.1111/j.1742-481X.2011.00923.x.

[5] G.R. Sibbald, H. Orsted, G.S. Schultz, P. Coutts, D. Keast, Preparing the wound bed: focus on infection and inflammation, Ostomy Wound Manag. 49 (2003) 24–51.

[6] J. Boateng, O. Catanzano, Advanced therapeutic dressings for effective wound healing – a review, J. Pharm. Sci. 104 (2015) 3653–3680, https://doi.org/10.1002/jps.24610.

[7] M. Gruppuso, G. Turco, E. Marsich, D. Porrelli, Polymeric wound dressings, an insight into polysaccharide-based electrospun membranes, Appl. Mater. Today 24 (2021), e101148, https://doi.org/10.1016/j.apmt.2021.101148.

[8] L. Wang, E. Khor, A. Wee, L.Y. Lim, Chitosan-alginate PEC membrane as a wound dressing: assessment of incisional wound healing, J. Biomed. Mater. Res. 63 (2002) 610–618, https://doi.org/10.1002/jbm.10382.

[9] D. Gopinath, M.R. Ahmed, K. Gomathi, K. Chitra, P.K. Sehgalb, R. Jayakumar, Dermal wound healing processes with curcumin incorporated collagen films, Biomaterials 25 (2004) 1911–1917, https://doi.org/10.1016/S0142-9612(03)00625-2.

[10] H.-E. Thu, M.H. Zulfakar, S. Fern Ng, Alginate based bilayer hydrocolloid films as potential slow-release modern wound dressing, Int. J. Pharm. 434 (2012) 375–383, https://doi.org/10.1016/j.ijpharm.2012.05.044.

[11] R. Pereira, A. Carvalho, D.C. Vaz, M.H. Gil, A. Mendes, P. Bártolo, Development of novel alginate based hydrogel films for wound healing applications, Int. J. Biol. Macromol. 52 (2013) 221–230, https://doi.org/10.1016/j.ijbiomac.2012.09.031.

[12] H. Li, Y. Xue, B. Jia, Y. Bai, Y. Zuo, S. Wang, Y. Zhao, W. Yang, H. Tang, The preparation of hyaluronic acid grafted pullulan polymers and their use in the formation of novel biocompatible wound healing film, Carbohydr. Polym. 188 (2018) 92–100, https://doi.org/10.1016/j.carbpol.2018.01.102.

[13] Y. Duan, K. Li, H. Wang, T. Wu, Y. Zhao, H. Lia, H. Tang, W. Yang, Preparation and evaluation of curcumin grafted hyaluronic acid modified pullulan polymers as a functional wound dressing material, Carbohydr. Polym. 238 (2020), e116195, https://doi.org/10.1016/j.carbpol.2020.116195.

[14] C. Chen, Y. Wang, D. Zhang, X. Wu, Y. Zhao, L. Shang, J. Ren, Y. Zhao, Natural polysaccharide based complex drug delivery system from microfluidic electrospray for wound healing, Appl. Mater. Today 23 (2021), e101000, https://doi.org/10.1016/j.apmt.2021.101000.

[15] H.V. Pawar, J. Tetteh, J.S. Boateng, Preparation, optimisation and characterisation of novel wound healing film dressings loaded with streptomycin and diclofenac,

Colloids Surf. B 102 (2013) 102–110, https://doi.org/10.1016/j.colsurfb.2012.08.014.

[16] U. Maver, L. Gradišnik, D.M. Smrke, K.S. Kleinschek, T. Maver, Impact of growth factors on wound healing in polysaccharide blend thin films, Appl. Surf. Sci. 489 (2019) 485–493, https://doi.org/10.1016/j.apsusc.2019.06.054.

[17] A. Ehteramia, M. Salehi, S. Farzamfar, H. Samadian, A. Vaez, S. Ghorbani, J. Ai, H. Sahrapeyma, Chitosan/alginate hydrogels containing Alpha-tocopherol for wound healing in rat model, J. Drug Deliv. Sci. Technol. 51 (2019) 204–213, https://doi.org/10.1016/j.jddst.2019.02.032.

[18] H.M. Fahmy, A.A. Aly, S.M. Sayed, A. Abou-Okeil, K-carrageenan/Na-alginate wound dressing with sustainable drug delivery properties, Polym. Adv. Technol. 32 (2021) 1793–1801, https://doi.org/10.1002/pat.5218.

[19] R.T. Selvi, A.P.S. Prasanna, R. Niranjan, M. Kaushik, T. Devasena, J. Kumar, R. Chelliah, D.-H. Oh, S. Swaminathan, G.D. Venkatasubbu, Metal oxide curcumin incorporated polymer patches for wound healing, Appl. Surf. Sci. 449 (2018) 603–609, https://doi.org/10.1016/j.apsusc.2018.01.143.

[20] R. Langer, Polymeric delivery systems for controlled drug release, Chem. Eng. Commun. 6 (1980) 1–48, https://doi.org/10.1080/00986448008912519.

[21] L. Li, R. Ni, Y. Shao, S. Mao, Carrageenan and its applications in drug delivery, Carbohydr. Polym. 103 (2014) 1–11, https://doi.org/10.1016/j.carbpol.2013.12.008.

[22] R. Yegappan, V. Selvaprithiviraj, S. Amirthalingam, R. Jayakumar, Carrageenan based hydrogels for drug delivery, tissue engineering and wound healing, Carbohydr. Polym. 198 (2018) 385–400, https://doi.org/10.1016/j.carbpol.2018.06.086.

[23] H.H. Tønnesen, J. Karlsen, Alginate in drug delivery systems, Drug Dev. Ind. Pharm. 28 (2002) 621–630, https://doi.org/10.1081/DDC-120003853.

[24] K. Varaprasad, T. Jayaramudu, V. Kanikireddy, C. Toro, E.R. Sadiku, Alginate-based composite materials for wound dressing application: a mini review, Carbohydr. Polym. 236 (2020), e116025, https://doi.org/10.1016/j.carbpol.2020.116025.

[25] D. Jain, D. Bar-Shalom, Alginate drug delivery systems: application in context of pharmaceutical and biomedical research, Drug Dev. Ind. Pharm. 40 (2014) 1576–1584, https://doi.org/10.3109/03639045.2014.917657.

[26] C.H. Goh, P.W.S. Heng, L.W. Chan, Alginates as a useful natural polymer for microencapsulation and therapeutic applications, Carbohydr. Polym. 88 (2012) 1–12, https://doi.org/10.1016/j.carbpol.2011.11.012.

[27] B. Cohen, A. Shefy-Peleg, M. Zilberman, Novel gelatin/alginate soft tissue adhesives loaded with drugs for pain management: structure and properties, J. Biomater. Sci. Polym. Ed. 25 (2014) 224–240, https://doi.org/10.1080/09205063.2013.849904.

[28] O. Pinkas, M. Zilberman, Effect of hemostatic agents on properties of gelatin–alginate soft tissue adhesives, J. Biomater. Sci. Polym. Ed. 25 (2014) 555–573, https://doi.org/10.1080/09205063.2014.881681.

[29] A. Shefy-Peleg, M. Foox, B. Cohen, M. Zilberman, Novel antibiotic-eluting gelatin-alginate soft tissue adhesives for various wound closing applications, Int. J. Polym. Mater. Polym. Biomater. 63 (2014) 699–707, https://doi.org/10.1080/00914037.2013.862535.

[30] K.Y. Lee, D.J. Mooney, Alginate: properties and biomedical applications, Prog. Polym. Sci. 37 (2012) 106–126, https://doi.org/10.1016/j.progpolymsci.2011.06.003.

[31] A.V. Kabanov, E.V. Batrakova, V.Y. Alakhov, Pluronic block copolymers as novel polymer therapeutics for drug and gene delivery, J. Control. Release 82 (2002) 189–212, https://doi.org/10.1016/S0168-3659(02)00009-3.

[32] G. Dumortier, J.L. Grossiord, F. Agnely, J.C. Chaume, A review of poloxamer 407 pharmaceutical and pharmacological characteristics, Pharm. Res. 23 (2006) 2709–2728, https://doi.org/10.1007/s11095-006-9104-4.

[33] W. Saski, S.G. Shah, Availability of drug in the presence of surface active agents. I. Critical micelle concentration of some oxyethylene–oxypropylene polymers, J. Pharm. Sci. 54 (1965) 71–74, https://doi.org/10.1002/jps.2600540117.

[34] K. Huang, B.P. Lee, D.R. Ingram, P.B. Messersmith, Synthesis and characterization of self-assembling block copolymers containing bioadhesive end groups, Biomacromolecules 3 (2002) 397–406, https://doi.org/10.1021/bm015650p.

[35] S.L. Percival, R. Chen, D. Mayer, A.-M. Salisbury, Mode of action of poloxamer-based surfactants in wound care and efficacy on biofilms, Int. Wound J. 15 (2018) 749–755, https://doi.org/10.1111/iwj.12922.

[36] R.A. Sharma, A.J. Gescher, W.P. Steward, Curcumin: the story so far, Eur. J. Cancer 41 (2005) 1955–1968, https://doi.org/10.1016/j.ejca.2005.05.009.

[37] Z. Stanić, Curcumin, a compound from natural sources, a true scientific challenge – a review, Plant Foods Hum. Nutr. 72 (2017) 1–12, https://doi.org/10.1007/s11130-016-0590-1.

[38] P. Anand, A.B. Kunnumakkara, R.A. Newman, B.B. Aggarwal, Bioavailability of curcumin: problems and promises, Mol. Pharm. 4 (2007) 807–818, https://doi.org/10.1021/mp700113r.

[39] A.S. Strimpakos, R.A. Sharma, Curcumin: preventive and therapeutic properties in laboratory studies and clinical trials, Antiox. Redox Signal 10 (2008) 511–546, https://doi.org/10.1089/ars.2007.1769.

[40] D. Akbik, M. Ghadiri, W. Chrzanowski, R. Rohanizadeh, Curcumin as a wound healing agent, Life Sci. 116 (2014) 1–7, https://doi.org/10.1016/j.lfs.2014.08.016.

[41] Sh.M. Abu-Bakr, N.M. Fawzy, S.A. Swelam, H.M. Awad, S.A. Ismail, Sh.A. Ismail, A.A. Aly, Green synthesis of curcumin derivatives with expected biological activities as potential antitumor, radical scavenging agents and their applications antibacterial wound dressings, Int. J. Green. Herb. Chem. 9 (2020) 199–209, https://doi.org/10.24214/IJGHC/GC/9/2/19909.

[42] B. Joe, M. Vijaykumar, B. Lokesh, Biological properties of curcumin-cellular and molecular mechanisms of action, Crit. Rev. Food Sci. Nutr. 44 (2004) 97–111, https://doi.org/10.1080/10408690490424702.

[43] M.A. da Silva, A.C.K. Bierhalz, T.G. Kieckbusch, Alginate and pectin composite films crosslinked with Ca2+ ions: Effect of the plasticizer concentration, Carbohydr. Polym. 77 (2009) 736–742, https://doi.org/10.1016/j.carbpol.2009.02.014.

[44] V. Paşcalău, V. Popescu, G.L. Popescu, M.C. Dudescu, G. Borodi, A. Dinescu, I. Perhaiţa, M. Paul, The alginate/k-carrageenan ratio's influence on the properties of the cross-linked composite films, J. Alloy. Compd. 536S (2012) S418–S423, https://doi.org/10.1016/j.jallcom.2011.12.026.

[45] P. Costa, J.M. Sousa Lobo, Modeling and comparison of dissolution profiles, Eur. J. Pharm. Sci. 13 (2001) 123–133, https://doi.org/10.1016/S0928-0987(01)00095-1.

[46] M.J. Frisch, G.W. Trucks, H.B. Schlegel, G.E. Scuseria, M.A. Robb, J.R. Cheeseman, G. Scalmani, V. Barone, B. Mennucci, G.A. Petersson, H. Nakatsuji, M. Caricato, X. Li, H.P. Hratchian, A.F. Izmaylov, J. Bloino, G. Zheng, J.L. Sonnenberg, M. Hada, M. Ehara, K. Toyota, R. Fukuda, J. Hasegawa, M. Ishida, T. Nakajima, Y. Honda, O. Kitao, H. Nakai, T. Vreven, J.A. Montgomery Jr., J.E. Peralta, F. Ogliaro, M. Bearpark, J.J. Heyd, E. Brothers, K.N. Kudin, V.N. Staroverov, R. Kobayashi, J. Normand, K. Raghavachari, A. Rendell, J.C. Burant, S.S. Iyengar, J. Tomasi, M. Cossi, N. Rega, J.M. Millam, M. Klene, J.E. Knox, J.B. Cross, V. Bakken, C. Adamo, J. Jaramillo, R. Gomperts, R.E. Stratmann, O. Yazyev, A.J. Austin, R. Cammi, C. Pomelli, J.W. Ochterski, R.L. Martin, K. Morokuma, V.G. Zakrzewski, G.A. Voth, P. Salvador, J.J. Dannenberg, S. Dapprich, A.D. Daniels, Ö. Farkas, J. B. Foresman, J.V. Ortiz, J. Cioslowski, D.J. Fox, Gaussian 09, Revision D.01, Gaussian, Inc., Wallingford CT, 2013.

[47] M.P.M. Costa, L.M. Prates, L. Baptista, M.T.M. Cruz, I.L.M. Ferreira, Interaction of polyelectrolyte complex between sodium alginate and chitosan dimers with a single glyphosate molecule: a DFT and NBO study, Carbohydr. Polym. 198 (2018) 51–60, https://doi.org/10.1016/j.carbpol.2018.06.052.

[48] A.E. Reed, L.A. Curtiss, F. Weinhold, Intermolecular interactions from a natural bond orbital, donor-acceptor viewpoint, Chem. Rev. 88 (1988) 899–926, https://doi.org/10.1021/cr00088a005.

[49] R.F.W. Bader, Atoms in molecules, Acc. Chem. Res. 18 (1985) 9–15, https://doi.org/10.1021/ar00109a003.

[50] T. Lu, F. Chen, Multiwfn: a multifunctional wavefunction analyzer, J. Comput. Chem. 33 (2012) 580–592, https://doi.org/10.1002/jcc.22885.

[51] S.F. Boys, F. Bernardi, The calculation of small molecular interactions by the differences of separate total energies. Some procedures with reduced errors, Mol. Phys. 19 (1970) 553–566, https://doi.org/10.1080/00268977000101561.

[52] T. Mosmann, Rapid colorimetric assay for cellular growth and survival: application to proliferation and cytotoxicity assays, J. lmmunol. Methods 65 (1983) 55–63, https://doi.org/10.1016/0022-1759(83)90303-4.

[53] L. Pham, L.H. Dang, M.D. Truong, T.H. Nguyen, L. Le, V.T. Le, N.D. Nam, L. G. Bach, V.T. Nguyen, N.Q. Tran, A dual synergistic of curcumin and gelatin on thermal-responsive hydrogel based on Chitosan-P123 in wound healing application, Biomed. Pharmacother. 117 (2019), e109183, https://doi.org/10.1016/j.biopha.2019.109183.

[54] J. Qu, X. Zhao, Y. Liang, T. Zhang, P.X. Ma, B. Guo, Antibacterial adhesive injectable hydrogels with rapid self-healing, extensibility and compressibility as wound dressing for joints skin wound healing, Biomaterials 183 (2018) 185–199, https://doi.org/10.1016/j.biomaterials.2018.08.044.

[55] J.S. Boateng, H.V. Pawar, J. Tetteh, Polyox and carrageenan based composite film dressing containing anti-microbial and anti-inflammatory drugs for effective

wound healing, Int. J. Pharm. 441 (2013) 181–191, https://doi.org/10.1016/j.ijpharm.2012.11.045.

[56] N. Laohakunjit, A. Noomhorm, Effect of plasticizers on mechanical and barrier properties of rice starch film, Starch/Stärke 56 (2004) 348–356, https://doi.org/10.1002/star.200300249.

[57] F. Kianfar, B.Z. Chowdhry, M.D. Antonijevic, J.S. Boateng, Novel films for drug delivery via the buccal mucosa using model soluble and insoluble drugs, Drug Dev. Ind. Pharm. 38 (2012) 1–14, https://doi.org/10.3109/03639045.2011.644294.

[58] S. Barbosa de Souza Ferreira, G. Braga, É. Lemos de Oliveira, H.C. Rosseto, N. Hioka, W. Caetano, M.L. Bruschi, Colloidal systems composed of poloxamer 407, different acrylic acid derivatives and curcuminoids: optimization of preparation method, type of bioadhesive polymer and storage conditions, J. Drug Deliv. Sci. Technol. 57 (2020), e101686, https://doi.org/10.1016/j.jddst.2020.101686.

[59] L.H. Dang, T.H. Nguyen, H.L.B. Tran, V.N. Doan, N.Q. Tran, Injectable nanocurcumin-formulated chitosan-g-pluronic hydrogel exhibiting a great potential for burn treatment, J. Healthc. Eng. 2018 (2018), e5754890, https://doi.org/10.1155/2018/5754890.

[60] D.T. Nguyen, V.T. Dinh, L.H. Dang, D.N. Nguyen, B.L. Giang, C.T. Nguyen, T.B. T. Nguyen, L.V. Thu, N.Q. Tran, Dual interactions of amphiphilic gelatin copolymer and nanocurcumin improving the delivery efficiency of the nanogels, Polymers 11 (2019), e814, https://doi.org/10.3390/polym11050814.

[61] K.T. Shalumon, K.H. Anulekha, S.V. Nair, K.P. Chennazhi, R. Jayakumar, Sodium alginate/poly(vinylalcohol)/nano ZnO composite nanofibers for antibacterial wound dressings, Int. J. Biol. Macromol. 49 (2011) 247–254, https://doi.org/10.1016/j.ijbiomac.2011.04.005.

[62] M. Rezvanain, N. Ahmad, M.C.I.M. Amina, S.-F. Ng, Optimization, characterization, and in vitro assessment of alginate-pectin ionic cross-linked hydrogel film for wound dressing applications, Int. J. Biol. Macromol. 97 (2017) 131–140, https://doi.org/10.1016/j.ijbiomac.2016.12.079.

[63] P. Ezati, J.W. Rhim, pH-responsive pectin-based multifunctional films incorporated with curcumin and sulfur nanoparticles, Carbohydr. Polym. 23 (2020), e115638, https://doi.org/10.1016/j.carbpol.2019.115638.

[64] S. Roy, J.-W. Rhim, Carrageenan-based antimicrobial bionanocomposite films incorporated with ZnO nanoparticles stabilized by melanin, Food Hydrocoll. 90 (2019) 500–507, https://doi.org/10.1016/j.foodhyd.2018.12.056.

[65] Y. Huang, N. Dan, W. Dan, W. Zhao, Reinforcement of polycaprolactone/chitosan with nanoclay and controlled release of curcumin for wound dressing, ACS Omega 4 (2019) 22292–22301, https://doi.org/10.1021/acsomega.9b02217.

[66] N. Wathoni, K. Motoyama, T. Higashi, M. Okajima, T. Kaneko, H. Arima, Enhancement of curcumin wound healing ability by complexation with 2-hydroxypropyl-γ-cyclodextrin in sacran hydrogel film, Int. J. Biol. Macromol. 98 (2017) 268–276, https://doi.org/10.1016/j.ijbiomac.2017.01.144.

[67] X. Li, K. Nan, L. Li, Z. Zhang, H. Chen, *In vivo* evaluation of curcumin nanoformulation loaded methoxy poly(ethylene glycol)-graft-chitosan composite film for wound healing application, Carbohydr. Polym. 88 (2012) 84–90, https://doi.org/10.1016/j.carbpol.2011.11.068.

[68] E. Espinosa, E. Molins, C. Lecomte, Hydrogen bond strengths revealed by topological analyses of experimentally observed electron densities, Chem. Phys. Lett. 285 (1998) 170–173, https://doi.org/10.1016/S0009-2614(98)00036-0.

[69] N.N. Karaush, G.V. Baryshnikov, V.A. Minaeva, B.F. Minaev, A DFT and QTAIM study of the novel d-block metal complexes with tetraoxa[8]circulene-based ligands, N. J. Chem. 39 (2015) 7815–7821, https://doi.org/10.1039/C5NJ01255D.

[70] A.V. Afonin, A.V. Vashchenko, M.V. Sigalov, Estimating the energy of intramolecular hydrogen bonds from 1H NMR and QTAIM calculations, Org. Biomol. Chem. 14 (2016) 11199–11211, https://doi.org/10.1039/C6OB01604A.